

Single-event-lumped-parameter hybrid (SELPH) model for non-ideal hydrocracking of *n*-octane

J.C. Chavarría-Hernández^a, J. Ramírez^{a,b,*}, M.A. Baltanás^c

^a UNICAT, Departamento de Ingeniería Química, Facultad de Química, UNAM. Cd. Universitaria, D.F., México

^b Instituto Mexicano del Petróleo, Eje Central Lázaro Cárdenas 152, D.F., 07730, México

^c INTEC, U.N.L.-CONICET, Güemes 3450-3000 Santa Fe, Argentina

Available online 3 December 2007

Abstract

Hydrocracking of normal octane was carried out at temperatures from 493 to 548 K and pressures of 15 and 35 bar. The experiments were performed on USY zeolite loaded with 0.25 wt.% Pt. The selected experimental conditions allowed a transition from ideal to non-ideal hydrocracking. Single-event kinetic rate constants were estimated in a first stage, using only the ideal-hydrocracking data and a single-event-ideal-hydrocracking model. The estimates of the first stage were used in a second stage in which a single-event-lumped-parameter hybrid (SELPH) model for non-ideal hydrocracking was used. The (SELPH) kinetic model was able to accurately describe the transition from ideal to non-ideal hydrocracking.

© 2007 Elsevier B.V. All rights reserved.

Keywords: Hydrocracking; Kinetic model; Single event; Non-ideal hydrocracking; SELPH model

1. Introduction

Hydrocracking is a catalytic hydroconversion process through which relatively heavy oil feedstocks are converted into lighter more valuable quality products such as gasoline, diesel, etc. [1]. Hydrocracking is a versatile process that takes place at high partial pressures of hydrogen. The process is performed on bifunctional zeolite catalysts that combine acidic and metal functions. Industrial catalysts commonly use Ni, Mo, Co or Pt supported on zeolite.

It is generally accepted [2] that the first step in the process is the adsorption of saturated hydrocarbons in the micropores of the zeolite, followed by the dehydrogenation on the metal sites to produce unsaturated species. The olefins formed migrate to the acid sites where they are protonated to produce carbenium ions, which in turn undergo acid-catalyzed isomerization and cracking reactions. The products of the cracking steps are also able to undergo isomerization and cracking transformations (secondary isomerization and cracking). Acid-catalyzed deprotonation of carbenium ions produce the corresponding olefins, which are in

turn hydrogenated on metal sites to the observable saturated products.

The balance between the metal and the acid functions of the catalyst is critical to the product selectivities observed in hydrocracking. If the activity of the metallic phase is sufficiently high to establish quasi-equilibrium of the (de)-hydrogenation reactions, then the acid-catalyzed reactions are the rate-determining steps. Under these conditions, the yield of the feed isomers reaches their maximum at any conversion level [3]. This behavior is currently referred to as ideal hydrocracking [4,5]. There is an “ideal-hydrocracking region” (i.e., a range of experimental variables in which the (de)-hydrogenation reactions are quasi-equilibrated), in which changes in the operating conditions do not affect the observed product selectivities. In this region, the products distribution is a unique function of the conversion [6,7].

If, on the other hand, the (de)-hydrogenation activity of the metal is not sufficiently high compared to the acid strength of the catalyst, then the selectivities of the reaction products will behave in a different way. In particular, the yield of feed isomers decreases and the yield of cracking products increases in comparison to the ideal case. Under non-ideal-hydrocracking conditions, the (de)-hydrogenation reactions could be the rate-determining steps.

* Corresponding author. Address: UNICAT, Departamento de Ingeniería Química, Facultad de Química, UNAM. Cd. Universitaria, D.F., México.

E-mail address: jrs@servidor.unam.mx (J. Ramírez).

Nomenclature

A_0	Arrhenius pre-exponential factor (h^{-1})
c	surface concentration ($\text{mol g}_{\text{cat}}^{-1}$)
c_{H^+}	free acid active sites concentration ($\text{mol g}_{\text{cat}}^{-1}$)
c_t	total concentration ($\text{mol g}_{\text{cat}}^{-1}$)
E_0	activation energy (kJ mol^{-1})
EQ	equilibrium
I^+	single carbenium ion
k	kinetic rate constant for an elementary reaction step (h^{-1})
k_{dh}	dehydrogenation kinetic rate constant (h^{-1})
k'	single-event kinetic rate constant (h^{-1})
K	equilibrium constant
K_L	Langmuir physisorption constant (bar^{-1})
K^{M}	chemisorption equilibrium constant ($\text{g}_{\text{cat}} \text{mol}^{-1}$)
LI^+	lump of carbenium ions
n_e	number of single events
o_k	single olefin ' k '
pH_2	hydrogen partial pressure (bar)
r	net production rate ($\text{mol g}_{\text{cat}}^{-1} \text{h}^{-1}$)
(s;s)	secondary–secondary
w_{jk}	weighting factors
y_{ij}	experimental response
\hat{y}_{ij}	calculated response

Superscripts

*	composite
A	acid sites
M	metal site

Subscripts

Cr	cracking reaction
dh	dehydrogenation
DB-	di-branched
De	deprotonation
H^+	free acid active sites
MB-	mono-branched
n-	normal
O_j	lump of olefins ' j '
PCP	isomerization via protonated cyclopropane
P_i	lump of paraffins ' i '
Pr	protonation
t	total

The variables affecting the “character” of hydrocracking have been recently studied. These variables include the operating conditions, the composition of the catalyst and the chain-length of the feed hydrocarbons. Specifically, it has been found that: (1) an increase in temperature, (2) a decrease of the total pressure [8], (3) the use of a weak hydrogenating function in the catalyst [9,10], (4) an increase of the chain-length of the feed hydrocarbon, and (5) an increase of the H_2 -to-hydrocarbon inlet molar ratio, enhance non-ideal hydrocracking [5].

Hydrocracking feedstocks commonly encountered in the oil refining industry contain a large number of hydrocarbons.

Kinetic modeling of the hydrocracking process required for simulation and optimization purposes is not a simple task. Early models were based on a drastic lumping of the chemical species involved [11]. A major disadvantage of such models is the dependence of the rate coefficients on the feed composition or reactor configuration.

The incorporation of the underlying chemistry for the individual hydrocarbons and the use of improved computational tools, made possible the development of the so-called fundamental models, which are able to give detailed information about the reaction products. The single-event model developed by Froment and coworkers [12,13] considers full detail of the reaction pathways of the individual feed components and reaction intermediates, expressing the kinetics of each reaction in terms of fundamental elementary steps.

The single-event kinetic approach has been applied successfully in the modeling of hydrocracking of single and complex feedstocks [14,15]. However, one of the basic assumptions of this approach has been that (de)-hydrogenation reactions are quasi-equilibrated. In the current terminology, this means that those models are restricted to ideal hydrocracking.

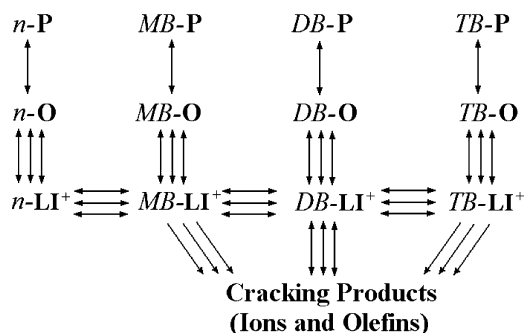
In the last few years, some attention has been devoted to the development of kinetic models that explicitly account for the non-ideal character of hydrocracking [5,10]. In the present work, the single-event methodology is applied in combination with the lumping approach to derive a hybrid kinetic model able to describe ideal and non-ideal hydrocracking. This work is in some way the continuation of a previous one in which the isothermal non-ideal hydrocracking of normal-hexadecane was modeled [10].

2. Kinetic model

The model described in this section was called single-event-lumped-parameter hybrid (SELPH) model because it combines two types of kinetic parameters: single-event-rate constants for the carbenium ion-reactions catalyzed on the acid sites, and lumped rate constants for the (de)-hydrogenation reactions on the metal sites.

2.1. Reaction network generation

The reaction network for the hydrocracking of n -octane, written in terms of elementary reaction steps, was generated using a computer program. In the program, every single hydrocarbon species is represented by a Boolean connectivity matrix [16]. The acid-catalyzed reactions considered in the generation of the reaction scheme are: protonation/deprotonation, hydride shift, methyl shift, PCP branching isomerization, and cracking in the β position with respect to the carbon atom bearing the positive charge. Only linear and branched species with a maximum of three branches were considered. This was in accordance with the reaction products observed in previously performed experiments. A total amount of 19 paraffins, 49 carbenium ions, and 58 olefins were considered in the reaction scheme. After the



Scheme 1. Lumped reaction scheme per carbon number.

complete reaction network generation, a lumping (relumping) approach was introduced for the acid-catalyzed reactions. This late-lumping does not affect the fundamental character of the single-event-rate constants. Each hydrocarbon species was lumped according to its nature (olefin or carbenium ion), number of carbon atoms and degree of branching. Scheme 1 shows the global lumped reaction scheme. Individual/lumps-of paraffins are also included. In it, n- stands for normal, MB- for mono-branched, DB- for di-branched, and TB- for tri-branched species, while P, O and LI⁺ indicate lumps of paraffins, olefins and carbenium ions, respectively.

2.2. Rate equations for the (de)-hydrogenation reactions

The transformation of paraffins into olefins is carried out on the metal sites of the catalyst. This process can be described in three steps: the chemisorption of the paraffins, the surface dehydrogenation reactions and desorption of the olefins formed.

Assuming a Rideal–Eley mechanism [17] with non-chemisorbed hydrogen, the rate at which the lump of paraffins, P_i , dehydrogenates into the corresponding lump of olefins, O_j , is given by

$$r_{\text{dh},P_i} = -k_{\text{dh},P_i} \cdot \left(c_{P_i}^M - \frac{c_{O_j}^M \cdot \text{pH}_2}{K_{\text{dh},P_i}} \right) \quad (1)$$

In Eq. (1), $c_{P_i}^M$ and $c_{O_j}^M$ are the adsorbed concentrations of the lumps of paraffins and olefins on metal sites.

It can be assumed that chemisorption reaches quasi-equilibrium and that the surface dehydrogenation reaction is the rate-determining step. Taken this assumption and using a Langmuir type isotherm to express the adsorbed concentrations of the lumps of paraffins and olefins, the previous equation is transformed to

$$r_{\text{dh},P_i} = \frac{-k_{\text{dh},P_i} \cdot K_{P_i}^M \cdot c_t^M \cdot (c_{P_i} - c_{O_j} \cdot \text{pH}_2 / (K_{P_i}^M / K_{O_j}^M)) \cdot K_{\text{dh},P_i}}{1 + \sum_i K_{P_i}^M \cdot c_{P_i}^M + \sum_j K_{O_j}^M \cdot c_{O_j}^M} \quad (2)$$

In Eq. (2) $K_{P_i}^M$ and $K_{O_j}^M$ are the chemisorption constants for the lumps of paraffins and olefins respectively, and c_t^M is the total concentration of the metal sites. It is convenient to define a

composite dehydrogenation rate constant as

$$k_{\text{dh},P_i}^* = \frac{k_{\text{dh},P_i} \cdot K_{P_i}^M \cdot c_t^M}{1 + \sum_i K_{P_i}^M \cdot c_{P_i}^M + \sum_j K_{O_j}^M \cdot c_{O_j}^M} \quad (3)$$

Substitution of Eq. (3) into Eq. (2) gives the following expression:

$$r_{\text{dh},P_i} = -k_{\text{dh},P_i}^* \cdot \left(c_{P_i} - \frac{c_{O_j} \cdot \text{pH}_2}{K'_{\text{dh},P_i}} \right) \quad (4)$$

with

$$K'_{\text{dh},P_i} = \frac{K_{P_i}^M}{K_{O_j}^M} \cdot K_{\text{dh},P_i} \quad (5)$$

In Eq. (4), the lumps of paraffins and olefins, P_i and O_j , respectively, are treated as single pseudo-components interconnected by a single reaction. This is represented in Scheme 1 by the use of single lines interconnecting the lumps of paraffins to the corresponding lumps olefins.

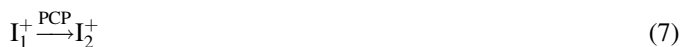
2.3. Rate equations for acid-catalyzed reactions

The kinetic equations for the acid-catalyzed reactions were derived by following the guidelines described in the single-event methodology [12,13]. Under this approach, the kinetic rate constant of an elementary reaction step, k in Eq. (6), is expressed as the product of the *single-event-rate constant* for that reaction step, k' , and a factor called *number of single events*, n_e .

$$k = n_e \cdot k' \quad (6)$$

Eq. (6) was derived using the definition of the transition state theory for the rate coefficient associated to an elementary reaction step. In Eq. (6), n_e accounts for the changes in symmetry (structure), occurring when the transition state is formed from the reactant species in an elementary reaction step. In this way, k' is assumed to depend only on the type of reaction (hydride shift, PCP branching, etc.) and the types of reactive and product carbenium ions (secondary or tertiary) involved in the reaction step. For example, $k'_{\text{PCP}(s;s)}$ denotes the single-event-rate constant for a PCP branching isomerization step in which a *secondary* carbenium ion produces another *secondary* carbenium ion. The contribution of primary carbenium ions are neglected in the reaction scheme since they are much more unstable than the secondary and tertiary ones.

The following example illustrates the way in which kinetic equations for the elementary reaction steps can be derived. Consider the left-to-right PCP-isomerization reaction between to single carbenium ions given as:



If both carbenium ions are secondary, then the net rate of formation of I_2^+ , is calculated in terms of the single-event-rate constant and the n_e value for that elementary step as

$$r_{I_2^+} = k'_{\text{PCP}(s;s)} \cdot n_e \cdot c_{I_1^+} \quad (8)$$

where $c_{I_1^+}$ is the adsorbed concentration of I_1^+ on acid sites.

In Scheme 1, the rate of the left-to-right isomerization between two lumps, say n-LI⁺ and MB-LI⁺ for example, is calculated as the sum of all the elementary isomerization reactions through which individual ions belonging to the first lump (n-LI⁺) produce individual ions belonging to the second lump (MB-LI⁺),

$$r_{\text{PCP}(n\text{-LI}^+ \rightarrow \text{MB-LI}^+)} = \sum_i n_{e,\text{PCP}_i} \cdot k'_{\text{PCP}}(m, u) \cdot c_{\text{I}_i^+} \quad (9)$$

In Eq. (9), m and u stand for the types of individual reactive and product carbenium ions, respectively. This kind of lumping is called relumping and is represented in Scheme 1 using triple lines interconnecting lumps of carbenium ions.

Analogous equations can be derived to calculate the rate at which the members of a lump of ions or the members of a lump of olefins are formed/consumed through β cracking reactions. Using explicit notation, the rate of disappearance of ions belonging to a lump of tri-branched species due to β cracking reactions is calculated as

$$r_{\text{Cr}(\text{TB-LI}^+)} = - \sum_i n_{e,\text{Cr}_i} \cdot k'_{\text{Cr}}(m, u) \cdot c_{\text{I}_i^+} \quad (10)$$

Accounting for all the isomerization and cracking reactions through which the elements of a lump of carbenium ions, LI⁺, are produced or consumed, the net rate of formation of that lump can be expressed in terms of equations of the types of (9) and (10) as

$$r_{\text{LI}^+} = \sum_s r_{\text{PCP},\text{LI}^+} + \sum_l r_{\text{Cr},\text{LI}^+} \quad (11)$$

where $r_{\text{PCP},\text{LI}^+}$ and $r_{\text{Cr},\text{LI}^+}$ are the net rates of formation of the elements of the lump of carbenium ions, LI⁺, due to PCP-isomerization and β cracking reactions.

Assuming protonation/deprotonation at quasi-equilibrium,



the net rate of formation of the lump of olefins, O_j on acid sites, is equal to the net rate of formation of the lump of carbenium ions, Eq. (11), with the same skeletal structure, plus the net rate at which olefins belonging to that lump (O_j) are formed through β cracking reactions:

$$r_{\text{O}_j\text{-acid}} = \sum_s r_{\text{PCP},\text{LI}^+} + \sum_l r_{\text{Cr},\text{LI}^+} + \sum_m r_{\text{Cr},\text{O}_j} \quad (13)$$

The third term on the right hand side of Eq. (13) only considers formation terms, since olefins do not disappear in cracking reactions.

The adsorbed concentrations of individual carbenium ions appearing implicitly or explicitly in Eqs. (8)–(11) and (13) are calculated in terms of the adsorbed concentrations of individual olefins (o_k), the free acid active sites, and the fundamental protonation and deprotonation rate constants as

$$c_{\text{I}_i^+} = K_{\text{Pr}/\text{De},k} \cdot c_{\text{O}_k} \cdot c_{\text{H}^+} = \frac{k_{\text{Pr}}(m)}{k_{\text{De}}(m, o_k)} \cdot c_{\text{O}_k} \cdot c_{\text{H}^+} \quad (14)$$

where m is the type of carbenium ion produced/consumed in the elementary protonation/deprotonation reaction.

The adsorbed concentrations of the individual olefins (o_k) appearing in Eq. (14) have to be expressed in terms of the adsorbed concentrations of the lumps of olefins to which they belong. This can be achieved by assuming quasi-equilibrium among the olefins that form a lump. This assumption can be valid for normal-, mono-branched- and even for di-branched-lumps, but is less valid for lumps of tri branched olefins [6,7]. Implementation of this assumption, allows calculating the net rate of formation of the lumps of olefins on acid sites, Eq. (13), in terms of the adsorbed concentrations of the lumps of olefins.

On the other hand, the net rate of formation of the lump of olefins O_j, due to (de)-hydrogenation reactions on metal sites is calculated using Eq. (4), rewritten as

$$r_{\text{O}_j\text{-metal}} = k_{\text{dh},\text{P}_i}^* \cdot \left(c_{\text{P}_i} - \frac{c_{\text{O}_j} \cdot \text{pH}_2}{K'_{\text{dh},\text{P}_i}} \right) \quad (15)$$

Finally, the net rate of formation of the lump of olefins O_j on acid and metal sites can be obtained from the sum of Eqs. (13) and (15).

$$r_{\text{O}_j} = r_{\text{O}_j\text{-acid}} + r_{\text{O}_j\text{-metal}} \quad (16)$$

Application of the pseudo-steady state approximation to the net rate of formation of the lumps of olefins gives:

$$r_{\text{O}_j} = r_{\text{O}_j\text{-acid}} + r_{\text{O}_j\text{-metal}} \quad (17)$$

Eq. (17) represents a set of linear equations, the solution of which gives the adsorbed concentrations of the lumps of olefins. Once these concentrations are known, the calculation of the net rate of disappearance of the lumps or paraffins is straightforward using Eq. (4).

2.4. Kinetic model simplifications

Further simplifying assumptions were introduced in the kinetic model, in order to facilitate its application:

- Since carbenium ions are re-lumped, type A isomerization reactions, i.e., hydride shift and methyl shift are assumed at quasi-equilibrium and no kinetic parameters have to be estimated for these steps.
- The simplifying assumptions and thermodynamic constraints commonly used in the application of the single-event approach [12,13] were implemented in the kinetic model. This led to an initial reduction in the number of independent single-event-rate constants to only 10: three for PCP-isomerization, three for β scission, two for protonation, and two for deprotonation.
- According to [14,18], it was found that concentration of free acid active sites approaches the total concentration of active acid sites; i.e., negligible adsorbed concentrations of carbenium ions are present. Implementation of this simplification in the model, leads to the replacement of c_{H^+} in Eq. (14) by the total active acid sites concentration, c_{t}^{A} .
- Estimation of independent protonation and deprotonation single-event-rate constants is eliminated by defining composite-single-event-rate constants for the PCP-isomerization

and β cracking steps, as follows:

$$k^* = k' \frac{k_{Pr}(u)}{k_{De}(u)} \cdot c_t^A \quad (18)$$

In Eq. (18) u is the type (secondary or tertiary) of the carbenium ion formed/disappeared in the protonation/deprotonation step, and k' is the single-event-rate constant for that PCP-isomerization or β cracking step. Eq. (18) implies the definition of the following composite pre-exponential factors and activation energies for the elementary isomerization and cracking reactions:

$$A_0^* = c_t^A \cdot A_0, \frac{A_{0,Pr}}{A_{0,De}} \quad (19)$$

$$E_a^* = E_a + \Delta H_{Pr} \quad (20)$$

In Eqs. (19) and (20) A_0 and E_a are the pre-exponential factor and the activation energy corresponding to a single-event-rate constant for a PCP-isomerization or a cracking step.

- Only one physisorption constant was used for the octane isomers. This was so, since for the first parameter estimation, no distinction could be made among isomers.
- Accounting for competitive adsorption, the physisorption constants for the cracked products were assumed zero.

With the simplifications described, the number of independent parameters to be estimated for the ideal-hydrocracking model of the first stage (see Section 3) was reduced to 14: 12 Arrhenius parameters for the six single-event-rate constants (three for PCP-isomerization and three for β cracking) and two parameters for the octane physisorption constant.

Additional simplifying assumptions were introduced in the SELPH kinetic model:

- The denominator of the right-hand-side of Eq. (3) was assumed constant and equal to unity. This assumption implies that the adsorbed concentrations of paraffins and olefins on the metal sites are negligible compared to the total available metal sites. Thybaut et al. [5] have found that this assumption is even more likely to be valid than the analogous one concerning the adsorption on acid sites.
- Only three octane lumps were retained in the final network: normal, mono-branched and di-branched. The amount of tri-branched species detected in the reaction products was negligible.

- In a preliminary parameter estimation, it was not possible to differentiate between some of the (de)-hydrogenation rate constants. For that reason, only one (de)-hydrogenation rate constant was retained for pentanes, and only one for butanes and propane.
- Finally, no appreciable catalyst deactivation was observed in the ideal- and non-ideal-hydrocracking experiments, so it was not necessary to include a deactivation function in the kinetic model. Implementation of the assumptions listed above, resulted in a total of 24 independent parameters to be adjusted for the SELPH model.

3. Strategy

In a first stage, a single-event-ideal-hydrocracking model was developed to estimate the single-event-rate parameters for PCP-isomerization and β cracking reactions. Only ideal-hydrocracking experimental data were used in the fitting of this stage.

In a second stage, the single-event-lumped-parameter hybrid (SELPH) model for non-ideal hydrocracking described in the preceding sections was developed. The experimental data used in the regression of the second stage correspond to ideal- and non-ideal-hydrocracking experiments.

The single-event estimates of the first stage were used as the initial estimates in the fitting of the second stage, since single-event parameters are assumed only catalyst dependent. The regression analysis of the second stage confirmed the validity of this assumption, since the values of the estimates increased a little but maintained the same order of magnitude respect to the values obtained with the single-event ideal model.

4. Experimental

The catalyst used in all the experiments was a USY zeolite with a Si/Al ratio of 30. Impregnation of 0.25 wt.% Pt with aqueous solution of H_2PtCl_6 was made using the pore volume method. Before the experiments, the catalyst was reduced in situ at 673 K during 4 h and under a flow of hydrogen of 60 ml/min. The experiments were performed in a stainless steel tubular reactor of 0.30 m length and 0.01 m internal diameter, equipped with automatic controllers of pressure and temperature. The catalyst particles were sized to 40–100 mesh (0.149–0.425 mm diameter) in order to eliminate diffusive effects. A feed consisting of H_2/n -octane mixture with a molar ratio of 100 was used in all the experiments.

Table 1
Ideal and non-ideal hydrocracking

Character of hydrocracking	P (bar)	T (K)	$(H_2/HC)^\circ$	W/F° ($g_{cat} \cdot h/mol$)	Kinetic model	
					Responses	Parameters
Ideal	35	493–523	100	50–250	8	14
Non-ideal	15	513–548	100	50–250	8	24

Operating conditions and number of independent parameters and responses for the ideal model and the more general non-ideal model.

The transition from ideal to non-ideal hydrocracking was achieved by varying pressure and temperature. Table 1 shows the experimental operating conditions for ideal and non-ideal hydrocracking. Liquid and gas reaction products were analyzed by gas chromatography. The identification of the products was achieved by GC–MS.

5. Results

The variation of the experimental conditions (T , P) allowed to transit from ideal- to non-ideal-hydrocracking behavior. The maximum conversion obtained in the experiments was about 50% for the ideal experiments and about 60% for the non-ideal experiments.

The responses (eight in each case) for both the ideal model in the first stage and the non-ideal model in the second stage, were the rates of formation of the lumps of paraffins. The optimization of the parameters was accomplished using a Levenberg–Marquardt algorithm, by minimization of the following objective function

$$S = \sum_{j=1}^{m_{\text{resp}}} \sum_{k=1}^{m_{\text{resp}}} w_{jk} \sum_{i=1}^{n_{\text{exp}}} (y_{ij} - \hat{y}_{ij})(y_{ik} - \hat{y}_{ik}) \quad (21)$$

where w_{jk} is the (j,k) element of the inverse of the covariance matrix of the experimental errors on the responses y .

Initial parameter estimates for both (ideal-hydrocracking and SELPH) models, were obtained from the modeling of isothermal and non-isothermal data at lower conversions requiring less number of parameters. Only the results of the fitting for the SELPH kinetic model are presented.

Table 2 lists the Arrhenius parameters for the composite single-event-rate constants, as well as those for the composite lumped (de)-hydrogenation rate constants. The value of the parameters for the octane Langmuir physisorption constant is also given.

Table 2
Estimates of the kinetic parameters for the SELPH model

	A_0^* (h^{-1})	E_a^* (kJ mol^{-1})
Single-event parameter		
$k_{\text{PCP}}^*(\text{s}; \text{s})$	3.45×10^{14}	60.8
$k_{\text{PCP}}^*(\text{s}; \text{t})$	1.77×10^{15}	71.6
$k_{\text{PCP}}^*(\text{t}; \text{t})$	5.91×10^{12}	51.7
$k_{\text{Cr}}^*(\text{s}; \text{s})$	4.73×10^{16}	82.6
$k_{\text{Cr}}^*(\text{s}; \text{t})$	1.08×10^{12}	25.4
$k_{\text{Cr}}^*(\text{t}; \text{s})$	1.73×10^{21}	92.0
Lumped parameter		
$k_{\text{dh},n-\text{P8}}^*$	6.4×10^{16}	64.5
$k_{\text{dh},\text{MB}-\text{P8}}^*$	2.8×10^{17}	25.5
$k_{\text{dh},\text{DB}-\text{P8}}^*$	3.1×10^{19}	39.6
$k_{\text{dh},\text{P5}}^*$	4.9×10^5	18.3
$k_{\text{dh},\text{P3P4}}^*$	6.1×10^6	21.5
Physisorption parameter		
	K_o (bar^{-1})	ΔH_{ads} (kJ mol^{-1})
$K_{\text{I-octanes}}$	6.24×10^{-3}	79.6

* Composite parameters.

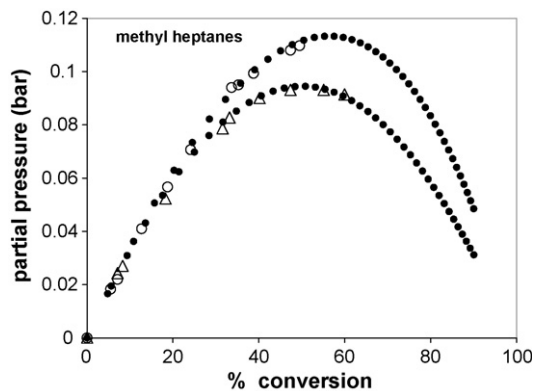


Fig. 1. Mono-methyl-heptanes partial pressure as a function of conversion: experimental (\circ ideal, \triangle non-ideal) and modeled (\bullet).

Figs. 1–4 show the comparison between two representative sets of experimental data: one set for the ideal-hydrocracking case and one for the non-ideal case. Figs. 1–3 show values of experimental partial pressure for some of the observed products, as a function of conversion, and the corresponding values calculated with the SELPH model. The experimental values correspond to the average of repeated experiments. As

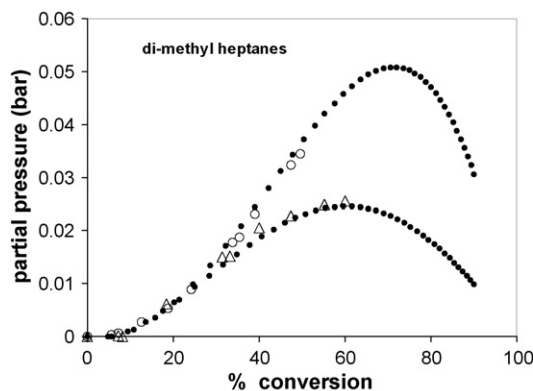


Fig. 2. Di-methyl-heptanes partial pressure as a function of conversion: experimental (\circ ideal, \triangle non-ideal) and modeled (\bullet).

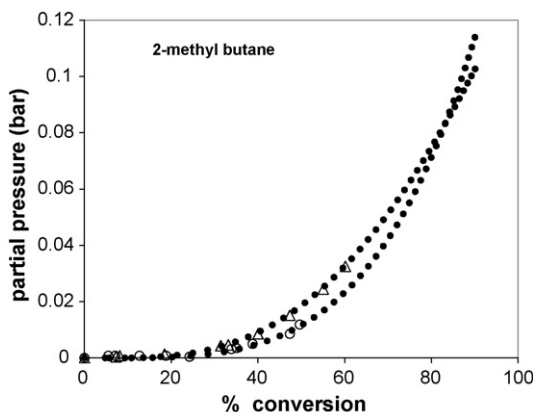


Fig. 3. 2-Methyl-butane partial pressure as a function of conversion: experimental (\circ ideal, \triangle non-ideal) and modeled (\bullet).

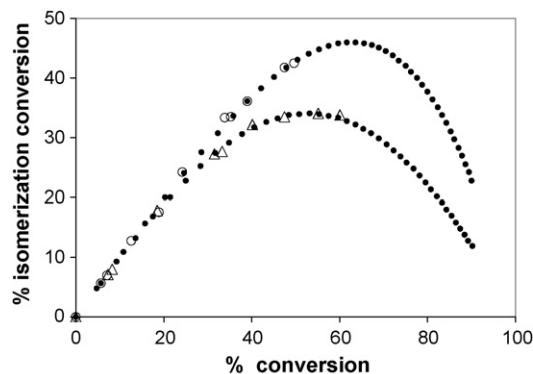


Fig. 4. Isomerization conversion vs. total conversion: experimental (○ ideal, △ non-ideal) and modeled (●).

can be appreciated, the model fits very well the experimental data.

Since no new types of reactions are expected to occur, the SELPH model is potentially able to estimate the expected behavior of the product distribution at conversion levels higher than the experimental ones. The product distribution trends calculated with the model are in accordance with experimental data at conversions higher than 60%, previously reported in the literature [7,8].

Fig. 4 shows the conversion towards isomerization as a function of total conversion. This figure is very useful in the examination of the ideal character of hydrocracking. In it, the lower the maximum in the curves, the higher the deviations from the ideal behavior.

6. Conclusions

The single-event-lumped-parameter hybrid (SELPH) model gives a good fitting of the experimental data. The kinetic model developed is capable of predicting with good accuracy the trends observed in the transition from ideal to non-ideal hydrocracking.

Single-event-rate parameters estimated with a single-event-ideal-hydrocracking model and ideal-hydrocracking experimental data can be used, with minor adjustments, to model non-ideal hydrocracking, using the SELPH model, with the condition that the same catalyst is used. This interesting result reinforces the statement that the single-event parameters are only catalyst dependent. This result can be used to greatly simplify the fitting task of the kinetic parameters of the SELPH kinetic model.

The character of hydrocracking is determined by the combination of several variables, including the operating conditions and the nature of the catalyst. In the present work, it was demonstrated that it is possible to transit from ideal to non-

ideal hydrocracking (or vice versa) by changing the operating temperature and pressure while using the same catalyst. This result illustrates the feasibility of the non-ideal hydrocracking (higher for longer chain-lengths of the feed hydrocarbons) and the importance of the development of non-ideal hydrocracking models.

Acknowledgments

We acknowledge financial support from the CONACyT (México)-SECYT (Argentina) program. JCCh acknowledges the scholarship granted by CONACyT-México.

References

- [1] I.E. Maxwell, J.K. Minderhoud, W.H. Stork, J.A.R. Van Veen, in: G. Ertl, H. Knozinger, J. Weitkamp (Eds.), *Hydrocracking and Catalytic Dewaxing in Handbook of Heterogeneous Catalysis*, vol. 4, Wiley-VCH, 1997, p. 2017.
- [2] J.A. Martens, P.A. Jacobs, in: J.B. Moffat (Ed.), *Conceptual Background for the Conversion of Hydrocarbons in Heterogeneous Acid Catalysts, Theoretical Aspects of Heterogeneous Catalysis*, Van Nostrand Reinhold, New York, 1990, p. 52.
- [3] F. Alvarez, F.R. Ribeiro, G. Perot, G. Thomazeau, M. Guisnet, *J. Catal.* 162 (1996) 179.
- [4] H. Schulz, J. Weitkamp, *Ind. Eng. Chem. Prod. Res. Dev.* 11 (1972) 46.
- [5] J.W. Thybaut, C.S. Laxmi Narasimhan, J.F. Denayer, G.V. Baron, P.A. Jacobs, J.A. Martens, G.B. Marin, *Catal. Lett.* 94 (1/2) (2004) 81.
- [6] M. Steijns, G.F. Froment, P. Jacobs, J. Uytterhoeven, J. Weitkamp, *Ind. Eng. Chem. Prod. Res. Dev.* 20 (1981) 654.
- [7] H. Vasina, M.A. Baltanás, G.F. Froment, *Ind. Eng. Chem. Prod. Res. Dev.* 22 (1983) 526.
- [8] D. Debrabandere, G.F. Froment, Influence of the hydrocarbon chain length on the kinetics of the hydroisomerization and hydrocracking of *n*-paraffins in hydrotreatment and hydrocracking of oil fractions, in: G.F. Froment, B. Delmon, P. Grange (Eds.), 1997, p. 379.
- [9] M.J. Girgis, Y.P. Tsao, *Ind. Eng. Chem. Res.* 35 (1996) 386.
- [10] J.C. Chavarría, J. Ramírez, H. González, M.A. Baltanás, *Catal. Today* 98 (2004) 235.
- [11] B.E. Stangeland, J.R. Kitrell, *Ind. Eng. Chem. Process. Des. Dev.* 11 (1972) 16.
- [12] M.A. Baltanás, K.K. Van Raemdonck, G.F. Froment, S.R. Mohedas, *Ind. Eng. Chem. Res.* 28 (1989) 899.
- [13] E. Vynckier, G.F. Froment, in: G. Astarita, S.I. Sandler (Eds.), *Kinetic and Thermodynamic Lumping of Multicomponent Mixtures*, Elsevier, Amsterdam, 1991, p. 131.
- [14] G.D. Svoboda, E. Vynckier, B. Debrabandere, G.F. Froment, *Ind. Eng. Chem. Res.* 34 (1995) 3793.
- [15] G.F. Froment, *Catal. Rev.* 47 (2005) 83.
- [16] M.A. Baltanás, G.F. Froment, *Comp. Chem. Eng.* 9 (1) (1985) 71.
- [17] R.I. Masel, *Principles of Adsorption and Reaction on Solid Surfaces*, John Wiley and sons, NY, 1996p.445.
- [18] M.A. Baltanás, H. Vasina, G.F. Froment, *Ind. Eng. Chem. Prod. Res. Dev.* 22 (1983) 531.